

03.1

## Infrared registration of the flame front of a hydrogen-air mixture propagating in porous copper

© G.Yu. Bivol, S.V. Golovastov, F.S. Kuleshov, V.V. Golub

Joint Institute for High Temperatures, Russian Academy of Sciences, Moscow, Russia  
E-mail: grigorij-bivol@yandex.ru

Received February 29, 2024

Revised March 20, 2024

Accepted March 20, 2024

Using a high-speed infrared camera, the propagation of a flame front in copper foam in hydrogen-air mixtures was studied. The copper foam of high permeability was used. The flame front propagation velocities and thermal radiation were determined, and the temperature of combustion products inside porous copper was evaluated. Microstructural and evaluative energy dispersive X-ray spectroscopy (EDS) of the surfaces of copper wire was carried out before the experiments and after the passage of the flame front.

**Keywords:** Copper foam, hydrogen, combustion, infrared registration, EDS.

DOI: 10.61011/TPL.2024.07.58716.19909

Close attention is paid at present to various applications of porous elements. Such elements are used to enhance the combustion efficiency and reduce harmful emissions [1] and for the design and fabrication of flame arresters and partitions of various purpose [2]. The use of porous metallic copper materials [3,4] with high permeability and low hydraulic resistance to extinguish the flame front is a relevant objective.

However, porous bodies with large pores may instead contribute to acceleration of the flame front. This acceleration may lead to supersonic combustion and the formation of shock waves [5,6]. The laws of filtration combustion have already been studied in sufficient detail. Combustion modes have been determined, and criteria for the transition from one mode to another have been established [7,8]. However, the difficulty of monitoring the flame front inside an optically opaque porous medium is noteworthy. The use of a high-speed infrared (IR) camera is one potentially efficient solution to this problem [9]. The aim of the present study is to monitor thermal radiation with an IR camera in the process of combustion of a hydrogen-air mixture in porous copper, estimate the temperature of combustion products during propagation in porous copper, and determine the surface composition of the copper frame.

Experiments were carried out in a channel open at both ends, which had an initiation section and a diagnostic section (Fig. 1). The initiation section with a circular cross-section 20 mm in diameter and a length of 665 mm featured a combustible mixture supply system and a spark gap. The energy of initiation by an electrical discharge was 0.1 J. The diagnostic section with a rectangular cross-section had transverse dimensions  $20 \times 16$  mm and a length of 200 mm. Side windows made of KI glass provided an opportunity to record the flame front in the IR range.

The hydrogen-air mixture was prepared in advance in a vessel  $3000 \text{ cm}^3$  in volume and mixed with a fan throughout

the entire duration of experiments (20–60 min). The volume concentration of hydrogen was 11, 14, and 20%. When the channel was filled with this flammable mixture, its left end was plugged. The volume of hydrogen-air mixture supplied into the channel ( $1500 \text{ cm}^3$ ) was 4 times greater than the channel volume. Following filling of the channel, the plug was removed. Experiments were performed at atmospheric pressure and a temperature of 295–298 K. The flame front inside porous copper was recorded by an Infratec ImageIR 8300 high-speed IR camera. The frame rate was 2000 frames per second at a resolution of  $348 \times 44$  pixels.

A porous copper sample 90 mm in length was positioned at a distance of 60 mm from the head of the diagnostic section. Porous copper with a density of 7 and 15 pores per inch (ppi) was used. The average fiber size and porosity were 0.6–0.8 mm and 97% for a pore density of 7 ppi and 0.4 mm and 97% for 15 ppi. Figure 1 shows the photograph of porous copper taken prior to experiments with a Nova NanoSem 650 scanning electron microscope.

Figure 2 presents a sequence of IR images forming an  $x-t$  diagram of flame front propagation upstream of porous copper, inside it, and downstream of porous copper. The presented results correspond to 11 vol.% of hydrogen and porous copper with a pore density of 7 ppi. The scale indicates the intensity of thermal radiation [ $\text{W/m}^2$ ] recorded by the IR camera. Figure 2 shows separate photographs of the perturbed flame front upstream of porous copper (1), the fragmented flame front inside porous copper (2), and the flame front after passing through porous copper (3). Time point  $t_0$  corresponds to the moment of transition of the flame front from the empty part of the channel into porous copper.

The change in slope of the tangent to the flame front trajectory in Fig. 2 suggests that the introduction of porous copper led to acceleration of the front. The flame front

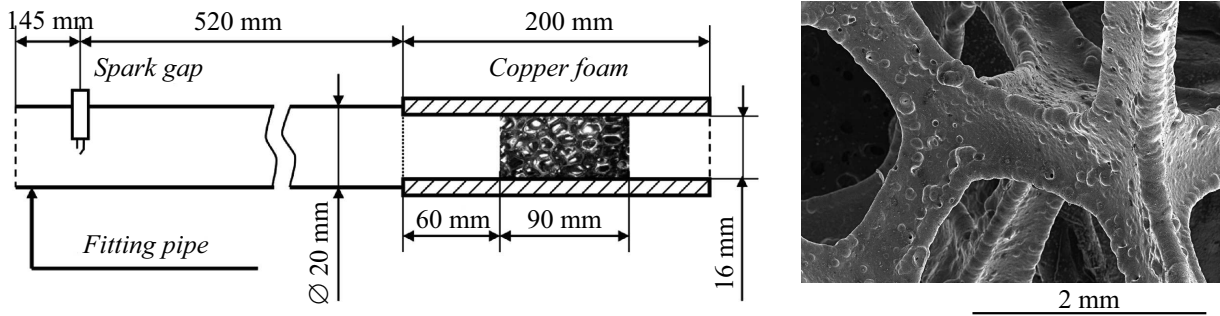


**Figure 1.** Diagram of the experimental setup and photographic image of porous copper with a pore density of 7 ppi.

**Table 1.** Characteristics of combustion of a hydrogen–air mixture in an empty channel and in porous copper

Hydrogen concentration, vol.%	Pore density, ppi	$I_0$ , W/m <sup>2</sup>	$I_{CF}$ , W/m <sup>2</sup>	$T_0$ , K	$T_{CF}$ , K	$(T_0 - T_{CF})/T_0$ , %	$\Delta T/T_0 = RT_0/E_s$ , % [10]
11	7	65 ± 4	61 ± 1	1178	1160 ± 30	1.44 ± 0.03	7
	15	52 ± 2	32 ± 2		1090 ± 80	7.7 ± 0.6	
14	7	120 ± 20	76 ± 4	1415	1200 ± 200	10 ± 2	9
	15	130 ± 10	90 ± 20		1300 ± 300	10 ± 2	
20	7	360 ± 20	290 ± 30	1833	1700 ± 100	6.2 ± 0.4	12
	15	399 ± 3	270 ± 20		1600 ± 100	12.1 ± 0.8	

velocities in the diagnostic section were determined based on the obtained images. This velocity was determined for the point on the flame front furthest from the spark gap. Figure 3 presents the variation of velocity corresponding to the three hydrogen concentrations used. Lower boundary  $v_{\min}$  is the minimum velocity in transition of the flame front from the empty part of the channel into porous copper, and upper boundary  $v_{\max}$  is the maximum velocity on exit of the flame front from the 90-mm-long porous copper sample. The flame front velocity is comparable to normal combustion velocity  $S$ . The exception to this rule is the mixture with a hydrogen concentration of 20 vol.%, since manifold acceleration of the front was induced in it by porous copper.

The intensities of thermal radiation of combustion products upstream of porous copper  $I_0$  and inside it  $I_{CF}$ , which are listed in Table 1, were determined based on the average maximum glow intensity of combustion products. The introduction of porous copper led to a reduction in radiation intensity due to heat exchange with the copper frame. When the hydrogen concentration increased from 11 to 20 vol.%, the thermal radiation intensity in porous copper grew from 32–60 to 270–290 W/m<sup>2</sup>.

Temperature  $T_{CF}$  of combustion products in the porous medium was estimated from intensity  $I$  of thermal radiation monitored with the IR camera. As was demonstrated earlier [11], intensity  $I$  of radiation recorded by the IR camera in the process of hydrogen combustion is related linearly to concentration  $n_{\text{H}_2\text{O},l}^e$  of excited water molecules. The

Boltzmann distribution allows one to estimate temperature  $T$  of these molecules:

$$I \sim n_{\text{H}_2\text{O},l}^e \sim n_{\text{H}_2\text{O}} \exp\left(-\frac{hc}{\lambda_l k_B T}\right), \quad (1)$$

where  $n_{\text{H}_2\text{O}}$  is the concentration of water molecules and  $\lambda_l = 2.74 \mu\text{m}$  is the vibrational excitation wavelength. Thus, the following is true in the approximation of complete combustion:

$$\frac{I_0 - I_{CF}}{I_0} \approx 1 - \exp\left[\frac{hc}{\lambda_l k_B} \left(\frac{1}{T_0} - \frac{1}{T_{CF}}\right)\right], \quad (2)$$

where  $T_0$  and  $T_{CF}$  are the temperatures of combustion in the empty channel and inside porous foam. Table 1 lists temperatures  $T_0$  of combustion products upstream of porous copper in the empty channel calculated from the energy balance for combustion products with the use of the IVTANTERMO code (Joint Institute for High Temperatures, Russian Academy of Sciences). The enthalpy of formation of water vapor in the gas phase was taken into account. It can be seen from Table 1, that the  $T_{CF}$  temperature reduction in porous copper calculated by Eq. (2) is 7.7–12.1% for a pore density of 15 ppi and 1.44–10% for a pore density of 7 ppi. These values corresponded to the maximum temperature reduction in adiabatic combustion [10].

The mass fractions of elements before the passage of the flame front and after 20 experiments in the hydrogen–air

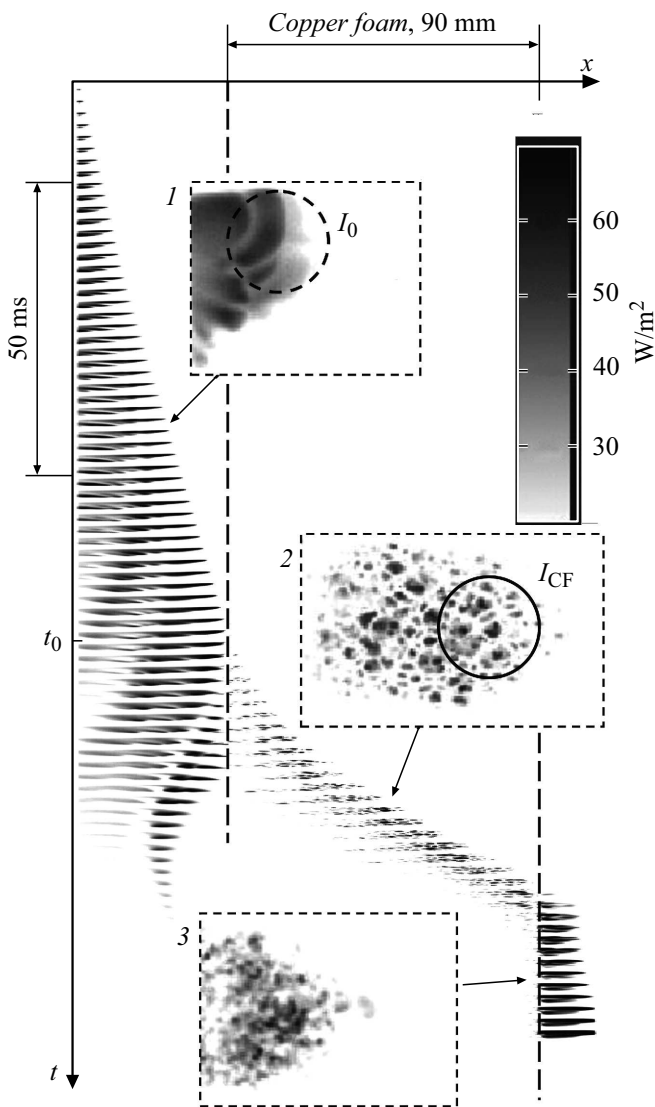


**Figure 2.**  $x-t$  propagation diagram and photographic images of the flame front upstream of porous copper (1), inside porous copper (2), and after passing through porous copper (3).  $I_0$  — thermal radiation intensity upstream of porous copper;  $I_{CF}$  — thermal radiation intensity inside porous copper.

mixture (Table 2) were determined by energy-dispersive X-ray spectroscopy (EDS) performed using a Nova NanoSem 650 scanning electron microscope. EDS analysis was carried out within surface regions  $100 \times 200 \mu\text{m}$  in size. It follows from Table 2 that the passage of the flame front leads to an increase in the mass fraction of oxygen on the copper surface, which grows from 2.2 to 2.9% after 20 experiments. Since the flame front width (0.4 mm) is comparable to the width of fibers of the copper frame (0.4–0.8 mm), heterogeneous reactions may raise the mass fraction of oxygen as a result of hydroxyl deactivation on the surface of the copper frame.

The obtained results suggest that the use of an IR camera allows one not only to determine the propagation velocity of the flame front of hydrogen–air mixtures in porous

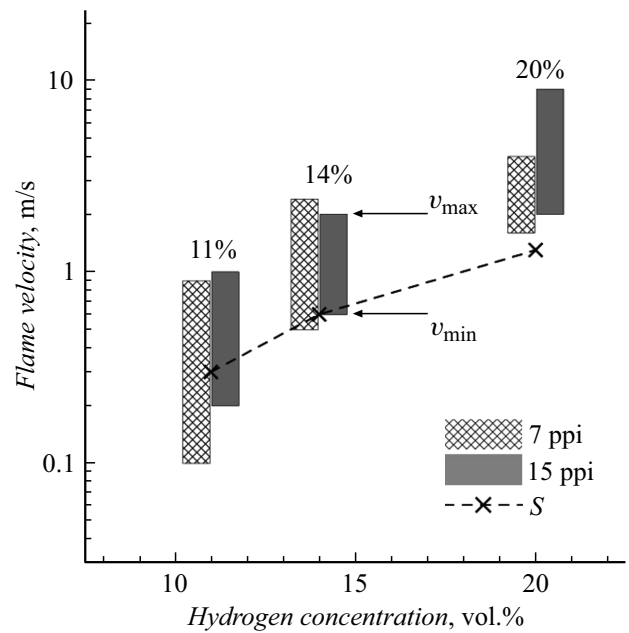


**Figure 3.** Variation of the flame front velocity in porous copper.  $S$  — normal velocity of flame propagation;  $v_{\min}$  and  $v_{\max}$  — minimum and maximum flame front velocities in porous copper.

**Table 2.** Mass fractions of elements before the experiments  $M_1$  and after (20 experiments) the passage of the flame front  $M_2$  (results of energy-dispersive analysis of the surface of porous copper)

Element	$M_1$ , mass%	$M_2$ , mass%
Cu	$93.0 \pm 0.9$	$92.0 \pm 0.7$
C	$2.9 \pm 0.4$	$2.8 \pm 0.9$
O	$2.2 \pm 0.4$	$2.9 \pm 0.6$
Fe	$0.5 \pm 0.2$	$0.5 \pm 0.2$
Al	$0.3 \pm 0.2$	$0.3 \pm 0.2$
Si	$0.3 \pm 0.1$	$0.5 \pm 0.3$
Ca	$0.2 \pm 0.1$	$0.4 \pm 0.2$
Other	$0.6 \pm 0.3$	$0.6 \pm 0.3$

copper, but also to perform quantitative measurements of transient thermal radiation and estimate the temperature of combustion products in the gas phase. The maximum temperature reduction varied from 1.44 to 12%. The results of EDS analysis are indicative of the hydroxyl nature of deactivation on the surface of the copper frame.

## Funding

This study was supported financially by the Russian Science Foundation, grant № 21-79-10363 (<https://rscf.ru/project/21-79-10363/>).

## Conflict of interest

The authors declare that they have no conflict of interest.

## References

- [1] Al.AI. Berlin, A.S. Shteinberg, S.M. Frolov, A.A. Belyaev, V.S. Posvyanskii, V.Ya. Basevich, Dokl. Phys. Chem., **406**, 43 (2006). DOI: 10.1134/S0012501606020059.
- [2] F. Cheng, J. Lu, T. Li, Z. Luo, J. Loss. Prevent. Process Ind., **78**, 104826 (2022). DOI: 10.1016/j.jlp.2022.104826
- [3] Y. Duan, F. Long, J. Long, S. Yu, H. Jia, Int. J. Hydrogen Energy, **48**, 22288 (2023). DOI: 10.1016/j.ijhydene.2023.03.157
- [4] K. Zheng, C. Song, Q. Jia, M. Fabrice, Z. Xing, X. Yang, Int. J. Hydrogen Energy, **50**, 829 (2024). DOI: 10.1016/j.ijhydene.2023.07.136
- [5] H.C. Li, R.W. Houim, Combust. Flame, **259**, 113118 (2024). DOI: 10.1016/j.combustflame.2023.113118
- [6] G.Yu. Bivol, S.V. Golovastov, V.V. Golub, N.K. Dentsel', A.E. El'yanov, F.S. Kuleshov, A.Yu. Mikushkin, A.A. Mikushkina, Gorenje Vzryv, **16** (2), 15 (2023) (in Russian). DOI: 10.30826/CE23160202
- [7] V. Babkin, A. Korzhavin, V. Bunev, Combust. Flame, **87**, 182 (1991). DOI: 10.1016/0010-2180(91)90168-B
- [8] V.I. Bubnovich, S.A. Zhdanok, K.V. Dobrego, Int. J. Heat Mass Transf., **49**, 2578 (2006). DOI: 10.1016/j.ijheatmasstransfer.2006.01.019
- [9] G.Yu. Bivol, S.V. Golovastov, V.V. Golub, Process Saf. Environ. Prot., **163**, 368 (2022). DOI: 10.1016/j.psep.2022.05.038
- [10] Ya.B. Zeldovich, G.I. Barenblatt, V.B. Librovich, G.M. Makhviladze, *Mathematical theory of combustion and explosion* (Plenum, N.Y., 1985).
- [11] G. Bivol, A. Gavrikov, V. Golub, A. Elyanov, V. Volodin, Exp. Therm. Fluid Sci., **121**, 110265 (2021). DOI: 10.1016/j.expthermflusci.2020.110265

*Translated by D.Safin*